Nanoparticle size determination using optical microscopes

Ravikiran Attota[*1], Premsagar Purushotham Kavuri[1], Hyeonggon Kang[1], Richard Kasica[2], and Lei Chen[2]

[1]*Semiconductor and Dimensional Metrology Division, NIST, Gaithersburg, MD 20899, USA*

[2]*Center for Nanoscale Science and Technology, NIST, Gaithersburg, MD 20899, USA*

**Corresponding author: ravikiran.attota@nist.gov*

Abstract: We present a simple method for size determination of nanoparticles using conventional optical microscopes. The method, called through-focus scanning optical microscopy (TSOM), makes use of the four-dimensional optical information collected at different focus positions. Low partial coherence illumination combined with analysis of through-focus optical content enables nanoparticle size determination with nanometer scale sensitivity. We experimentally demonstrate this using fabricated Si nanodots and spherical gold nanoparticles. The method is economical, as no hardware modifications to conventional optical microscopes are needed. In addition, the method also has high throughput and potential for soft nanoparticle size determination without distortion.

There is a great interest in using nanoparticles [1-8] because of their variety of biological applications, such as gene and drug delivery [1,2], imaging [3,4], and biosensing [5,6]. Size of the nanoparticles is a critical factor for their effective biological application [7]. Although there are several tools available for size determination of nanoparticles [7-12], there is a concern that most of the available high-throughput methods have insufficient level of accuracy as per the definition of particle size distribution by the National Institute of Standards and Technology [7,13]. In addition, there is also a concern that “soft” or “fuzzy” nanoparticles are difficult to characterize using high-resolution methods such as transmission electron microscopy (TEM) or scanning electron microscopy (SEM), since these methods deform nanoparticles during the measurement process. The most widely used dynamic light scattering (DLS) method also has several limitations such as systematic offset compared with TEM measurements [7]. Single-particle counting methods such as nanoparticle tracking analysis (NTA) and scanning ion occlusion sensing (SIOS) were found to be superior to DLS [14].

Although optics-based methods have the advantage of high-throughput, conventional optical microscopes have not been seriously considered so far for size determination of nanoparticles, perhaps, due to perceived diffraction limits. However, using the smallest condenser aperture (i.e. using low partial coherence), nanoparticles as small as 3 nm in diameter were clearly imaged (including through-focus images) using conventional bright-field optical microscopes [15,16]. On the other hand, increasing condenser aperture diameter to normal operating diameter (i.e. using high partial coherence) nanoparticles could not be imaged. The increased coherence condition enabled clearer imaging of nanoparticles. Through-focus optical images under the low partial coherence condition were successfully used to track motion of the nanoparticles with axial, lateral and temporal resolutions of 50 nm, 5 nm and 200 ms, respectively [17]. However, optical microscopes are not yet used for nanoparticle size determination. In this article, we present a single-particle counting method to determine size of nanoparticles using widely available conventional optical microscopes without complicated modifications to the optics or hardware. We propose a method that simply makes use of the through-focus optical data for size determination. An added advantage of this method is the potential ability to determine the size (including soft-nanoparticles), or changes in the size of nanoparticles in their native state without distortion with nanometer scale resolution.

In conventional optical microscopy, it is usually deemed necessary to acquire images at the "best focus" position. However, the out-of-focus images do contain additional useful information regarding the

target. The through-focus scanning optical microscopy (TSOM--pronounced as 'tee-som') imaging method introduced in 2006 [18-25] enables harnessing this additional information. A TSOM image is constructed from the four-dimensional (4-D) optical data [25] acquired using a conventional optical microscope as a target is scanned along the focus direction [20,22]. A multimedia figure depicts this process in Fig.1. In the TSOM image the X (horizontal), Y (vertical), and color scale axes represent the spatial position across the target, the focus position, and the optical intensity, respectively. We make use of the optical content of a TSOM image for size determination of nanoparticles. We chose two methods of quantifying the optical content of a TSOM image. The first method is the mean square intensity (MSI) defined as:

$$MSI = \frac{1}{n}\sum_{i=1}^{n}(A_i)^2$$

where A_i represents the ith pixel of a TSOM image A and n is the total number of pixels in A. The second method is the optical intensity range (OIR) [24] defined as the absolute difference between the maximum and the minimum optical intensity in a given TSOM image multiplied by 100. In the current paper we demonstrate the usefulness of both the MSI and the OIR for size determination of nanoparticles.

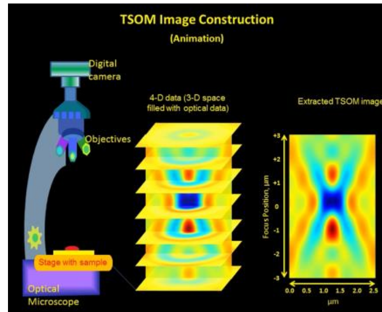

Fig. 1. An animation showing the construction method of a TSOM image (multimedia view).

Conventional microscopy suggests high numerical aperture (NA) (high partial coherence) for enhanced optical image resolution. However, improved ability to image nanoparticles was demonstrated using low partial coherence [15]. For this reason in the following work we use low partial coherence for size determination.

Nanodots of various sizes were fabricated using semiconductor technology. They were designed such that the side length of the top square varied from 50 nm to 200 nm (Fig. 2(a)), with a constant height. Post-fabrication metrology carried out using an SEM was used in this study as reference measurement (nominal measurement uncertainty of about 5%). A typical top-down SEM image is shown in Fig. 2(b). The height of the nanodots was measured using atomic force microscope and found to have a near constant value of about 71 nm.

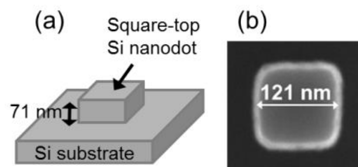

Fig. 2. (a) Schematic of a nanodot. (b) Top-down SEM image of a 121 nm nanodot.

Through-focus optical images of the fabricated nanodots for TSOM analysis were acquired using a conventional, bright-field, optical microscope in the reflection mode. A mercury-vapor lamp with band-pass filter produced a 546 nm wavelength illumination (unpolarized). Two illumination NAs of 0.1 and 0.27 were used with a 0.8 collection NA objective resulting in partial coherence factors (σ) of 0.125 and 0.337, respectively. A through-focus step height of 200 nm and a scan range of 10 μm were used during the data acquisition. The through-focus optical images were analyzed using an in-house developed software program [24,25]. Measurements were repeated at least three times.

In a second experiment spherical gold (Au) nanoparticles dispersed on Si substrate were analyzed using a second optical microscope. Unpolarized LED illumination (using a band-pass filter) at 520 nm was used with a σ value of 0.176 (illumination NA=0.15 and collection NA=0.85). A through-focus step height of 200 nm and a scan range of 12 μm were used during the data acquisition.

Following the size measurement of the nanodots with SEM, the TSOM images were acquired for the selected nanodots. Typical experimental through-focus optical images of a 121 nm nanodot are shown in Fig. 3(a) at three different focus positions. From the images it can be observed that the optical image response of the nanodots changes considerably depending on the focus position. The core appears either bright or dark based on the focus position. Determination of the best focus position is ambiguous under the experimental conditions used because of the clear, high contrast images at the two focus positions. TSOM image constructed from the set of through-focus optical images is shown in Fig. 3(b) at a σ of 0.125. The red lines marked on the TSOM image depict the focus positions of the optical images shown in Fig. 3(a). Optical intensity plots indicating reversal of intensity with focus are shown in Fig. 3(c). The TSOM image appears drastically different from a typical optical image. To better understand the concept of the TSOM image, the relative orientations of the optical image plane and the TSOM image plane are shown in Fig. 3(d). TSOM image of the 143 nm nanodot shown in Fig. 3(e) appears strikingly similar to the TSOM image of 121 nm size nanodot shown in Fig. 3(b). However, the optical content as observed by the color scale bar (OIR) increased. TSOM images at a σ of 0.337 are shown in Figs. 4(a) and (b). They appear different from the TSOM images shown in Fig. 3, but show strong similarity in the pattern (within themselves) along with increased OIR as a function of the nanodot size.

From both Figs. 3 and 4, increased optical content of the TSOM images and similar pattern (for a given σ) can be observed with increased size of the nanodots. We are able to make use of both the MSI and the OIR to quantify the changing optical content and subsequently measure size of the nanodots. To demonstrate this, first optical content was extracted for the selected nanodots using MSI and OIR for σ values of 0.125 and 0.337, respectively, and plotted as a function of the nanodot size as shown in Fig. 5. Under the current experimental conditions both the curves nominally follow a linear trend. These two plots are treated as the library, or the calibration curves for size determination of nanodots of unknown size. Using these calibration curves, an attempt was made to measure the size of a test nanodot, the size of which was previously measured to be 103 nm using the SEM, but not included in the creation of the calibration curves. The MSI and the OIR values of the TSOM image of the test nanodot were then compared with the calibration curves as shown in Fig 5, producing measured sizes of 108 nm and 106 nm, respectively. Following a similar procedure nanodot sizes can be determined using calibrated curves.

Applicability of the same procedure was tested for spherical Au nanoparticles also. Using an SEM, spherical-shaped Au nanoparticles were identified and their sizes were measured. Since the shape of the Au nanoparticles varies considerably, it is important to select nearly-spherical nanoparticles for the calibration curve. The identified Au nanoparticles were then analyzed using the TSOM method. OIR values from the TSOM images were plotted as a function of the SEM-measured mean particle diameters. A fitted curve using these values results in a calibration curve (or library) as shown in Fig. 6 for the Au nanoparticles under the experimental conditions used. The 156 nm diameter nanoparticle was considered as a test target and hence its value was not included in the calibration curve. The size of the test target was measured by comparing its OIR value with the calibration curve. As shown in Fig. 6, the TSOM-measured diameter is 153 nm.

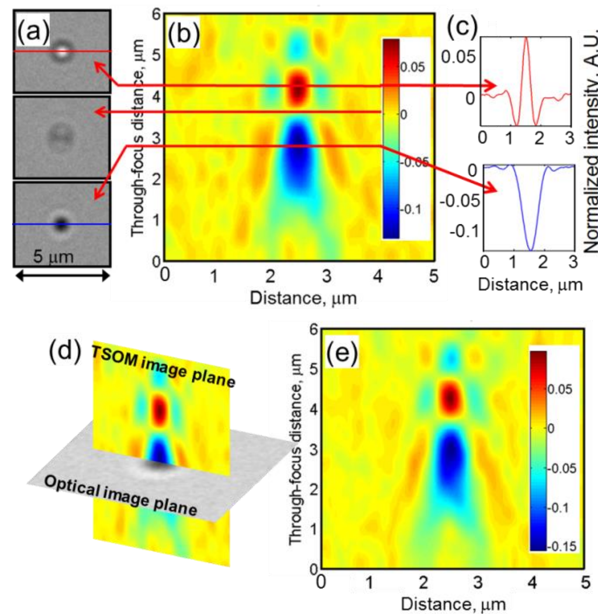

Fig. 3. (a) Optical images of a 121 nm nanodot at the three focus distances. (b) Experimental intensity normalized TSOM image of a 121 nm nanodot depicting the focus distances at which the optical images in (a) are extracted. (c) Optical intensity profiles at the two focus positions indicated by the arrow marks. Locations of the intensity profiles are marked on the optical images shown in (a) as red and blues lines. (d) Optical and TSOM image planes showing their relative orientations. (e) Experimental intensity normalized TSOM image of a 143 nm nanodot. Wavelength = 546 nm, σ = 0.125, Si nanodot on Si substrate.

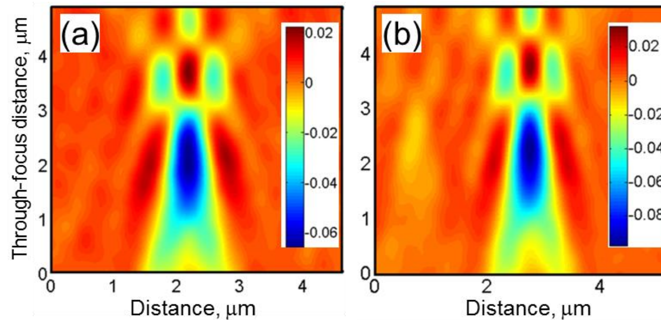

Fig. 4. Experimental intensity normalized TSOM images of (a) 121 nm, and (b) 143 nm nanodots. Wavelength = 546 nm, σ = 0.337, Si nanodot on Si substrate.

The current study is comparable to the literature in terms of improved ability to image nanoparticles with lower partial coherence (by reducing condenser aperture) [15]. As expected we have observed that decreasing σ from 0.337 to 0.1 increased OIR (i.e. optical intensity) of the TSOM images from 8.5 to 20 for a 121 nm nanodot (Figs. 3 and 4). On the other hand, lower σ values (as used in the current study) also produce optical interactions along a larger focus distance. The TSOM method makes it convenient to study and obtain meaningful information about these enhanced optical interactions.

In this paper size determination of nanodots and nanoparticles has been experimentally demonstrated using the same TSOM method. However, calibration curves can be different based on the type of nanoparticles (such as shape, material) and also experimental conditions (such as illumination and collection NAs, illumination wavelength).

The measured size difference between the SEM and the TSOM method falls within the SEM measurement uncertainty of 5%. Measurement resolution of the TSOM method was shown to be a nanometer or less [25]. Similar measurement resolutions can be expected in the case of nanodots/nanoparticles as well. The method is effective only if an acceptable quality database of TSOM images is available.

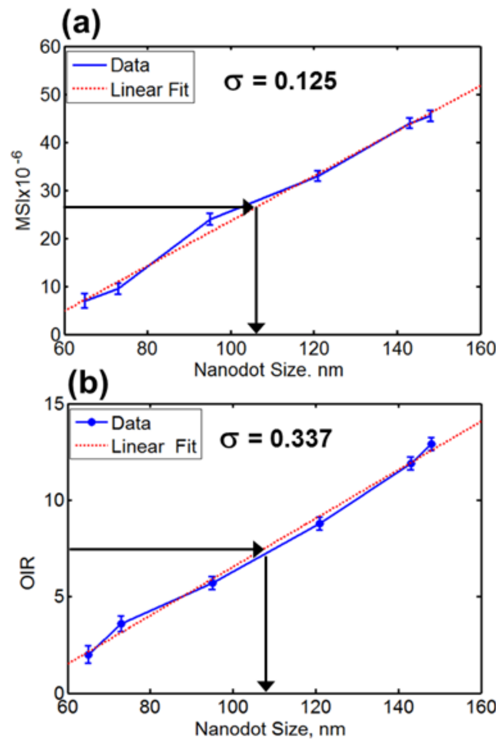

Fig. 5. Experimental (a) mean square intensities (MSI) for σ = 0.125, and (b) optical intensity ranges (OIR) for σ = 0.337 of the normalized TSOM images collected from the set of fabricated square nanodots showing a linear trend with size (within the size range tested). Arrow marks indicate determination of the unknown size of a nanodot using the library.

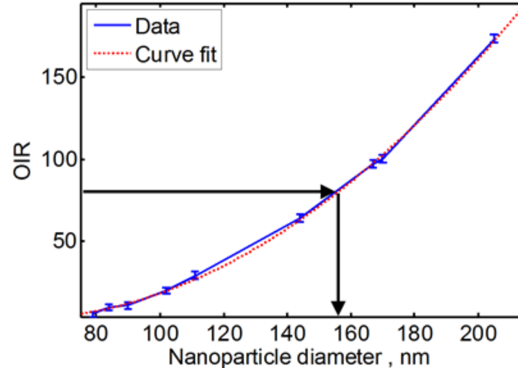

Fig. 6. Calibration curve generated using the measured TSOM images of spherical Au nanoparticles on a Si substrate. Arrow marks indicate size determination of an "unknown" spherical Au nanoparticle using the OIR value of the TSOM image. Wavelength = 520 nm, σ = 0.176 (Illumination NA = 0.15, collection NA = 0.85).

Limitations of this method include optical isolation of a nanoparticle from its nearest neighbor. The isolation distance is preferably over 2 to 4 times the illumination wavelength. Another limitation is that the substrate on which particles rest should be optically smooth. Alternatively, the particles could be suspended or trapped in a clear high-viscous solution or gel. The OIR value reaches saturation as the particle size increases. For this reason, use of the OIR may be limited to smaller sized nanoparticles. However, MSI could be used for a larger size range.

The library-matching TSOM method requires no specialized tools or hardware. Any optical microscope with adequate focus control is sufficient. The method is also amenable to a wide variety of sample material types as long as there is sufficient optical contrast between the nanoparticles (or nanoscale volume) and the surrounding media (or substrate). It could also be applied to analyze fluorescent particles. It can be used in both reflection (as in the current study) and transmission [15] optical modes. Since it does not require a best-focus position, several particles in the field-of-view can be analyzed simultaneously even if they are positioned at different heights, as long as they are trapped in a transparent liquid or gel and they are not optically interacting with each other.

Since the TSOM method is based on optical microscopes, it is economical, has high throughput, and is non-contacting, non-deforming and non-contaminating. High throughput is achieved in two ways: short measurement times (200 ms) [17], and the ability to simultaneously measure several nanoparticles located in the field of view, including at different heights. Ubiquitous optical microscopes will likely help this method to be implemented readily, especially for quality control.

In summary, low partial coherence illumination enabled improved imaging of the fabricated prismatic Si nanodots and Au nanoparticles using conventional optical microscopes. The TSOM method was used to analyze through-focus optical content of the nanodots and nanoparticles. Under the range of sizes tested, optical content evaluated using both the mean square intensity (MSI) and the optical intensity rage (OIR) increased with size. We demonstrated the size determination of nanodots and nanoparticles using calibration curves generated using MSIs and OIRs. Implementation of the same procedure enables nanoparticle size determination of any material. With appropriate experimental conditions nanoparticle sizes as small as 3 nm [15] could be determined using the TSOM library matching method.

Acknowledgements

The authors would like to thank Andras Vladar for providing access to an SEM and Rick Silver for providing access to an optical microscope.

References

1. J. Panyam, and V. Labhasetwar, Adv. Drug Deliv. Rev. **55,** 329 (2003).
2. N. Kohler, C. Sun, J. Wang, and M. Zhang, Langmuir **21**, 8858 (2005).
3. W. C. Chan, and S. M. Nie, Science **281**, 2016 (1998).
4. W. Jiang, E. Papa, H. Fischer, S. Mardyani, and W. C. W. Chan, Trends Biotechnol. **22**, 607 (2004).
5. M. Karhanek, J. T. Kemp, N. Pourmand, R. W. Davis, and C. D. Webb, Nano Lett. **5**, 403 (2005).
6. I. L. Medintz, A. R. Clapp, J. S. Melinger, H. T. Uyeda, J. R. Deschamps, and H. Mattoussi, Adv. Mater. **17**, 2450 (2005).
7. A. Wei, J. G. Mehtala, and A. K. Patri, J. Control. Release **164**, 236 (2012).
8. B. J. Berne, and R. Pecora, Dover Publications, Inc. New York (2000).
9. M. Felix, T. Klein, E. Buhr, C. G. Frase, G. Gleber, M. Krumrey, A. Duta, S. Duta, V. Korpelainen, R. Bellotti, Meas. Sci. Technol. **23**, 125005 (2012).
10. C. Pache, N. L. Bocchio, A. Bouwens, M. Villiger, C. Berclaz, J. Goulley, M. Gibson, C. Santschi and T. Lasser, Opt. Express **20**, 21385 (2012).
11. S. B. Rice, C. Chan. S. C. Brown, P. Eschbach, L. Han, D. S. Ensor, A. B. Stefaniak, J. Bonevich, A. E. Vladár, A. R. H. Walker, Metrologia 50 (6), 663 (2013).
12. R. I. MacCuspie, K. Rogers, M. Patra, Z. Suo, A. J. Allen, M. N. Martin, and V. A. Hackley, J. Environmental Monitoring 13 (5), 1212 (2011).
13. S. Xu, Z. Nie, M. Seo, P. Lewis, E. Kumacheva, H. A. Stone, P. Garstecki, D. B. Weibel, I. Gitlin, and G. M. Whitesides, Angew. Chem. Int. ed. **44**, 724 (2005).
14. N. C. Bell, C. Minelli, J. Tompkins, M. M. Stevens, and A. G. Shard, Langmuir **28**, 10860 (2012).
15. E. A. Patterson, and M. P. Whelan, Small **4**, 1703 (2008).
16. E. A. Patterson, and M. P. Whelan, Nanotechnology 19, 105502 (2008).
17. J. M. Gineste, P. Macko, E. A. Patterson and M. P. Whelan, J. Microscopy **243**, 172 (2011).
18. R. Attota, R. M. Silver, and J. Potzick, Proc. SPIE **6289**, 62890Q-1-10 (2006).
19. R. Attota, T. A. Germer, and R. M. Silver, Opt. Lett. **33**, 1990 (2008).
20. R. Attota, and R. M. Silver, Meas. Sci. Technol. **22**, 024002, (2011).
21. R. Attota, R. G. Dixson, J. A. Kramar, J. E. Potzick, A. E. Vladar, B. Bunday, A. Rudack, and E. Novak, Proc. SPIE **7971**, 79710T (2011).
22. R. Attota, R. Kasica, L. Chen, P. Kavuri, R. Silver and A. Vladar, Proc. Nanotech **2010**, 880 (2010).
23. B. Damazo, R. Attota, P. Kavuri and A. Vladar, Proc. SPIE **8324**, 832436 (2012).
24. R. Attota, B. Bunday and V. Vartanian, Appl. Phys. Lett. **102**, 222107 (2013).
25. R. Attota and R. G. Dixson, Appl. Phys. Lett. **105**, 043101 (2014).